HHS Public Access

Author manuscript

Exp Neurol. Author manuscript; available in PMC 2019 May 01.

Published in final edited form as:

Exp Neurol. 2018 May ; 303: 1–11. doi:10.1016/j.expneurol.2018.01.019.

Dissipation of transmembrane potassium gradient is the main cause of cerebral ischemia-induced depolarization in astrocytes and neurons

Yixing Du[a], **Wei Wang**[a,b], **Anthony D. Lutton**[c], **Conrad M. Kiyoshi**[a], **Baofeng Ma**[a], **Anne T. Taylor**[a], **John W. Olesik**[c], **Dana M. McTigue**[a], **Candice C. Askwith**[a], and **Min Zhou**[a,*]

[a]Department of Neuroscience, The Ohio State University Wexner Medical Center, Columbus, OH 43210, USA

[b]Department of Physiology, School of Basic Medicine, Huazhong University of Science and Technology, Wuhan 430030, China

[c]Trace Element Research Laboratory, The Ohio State University, Columbus, OH 43210, USA

Abstract

Membrane potential (V_M) depolarization occurs immediately following cerebral ischemia and is devastating for the astrocyte homeostasis and neuronal signaling. Previously, an excessive release of extracellular K^+ and glutamate has been shown to underlie an ischemia-induced V_M depolarization. Ischemic insults should impair membrane ion channels and disrupt the physiological ion gradients. However, their respective contribution to ischemia-induced neuronal and glial depolarization and loss of neuronal excitability are unanswered questions. A short-term oxygen-glucose deprivation (OGD) was used for the purpose of examining the acute effect of ischemic conditions on ion channel activity and physiological K^+ gradient in neurons and glial cells. We show that a 30 min OGD treatment exerted no measurable damage to the function of membrane ion channels in neurons, astrocytes, and NG2 glia. As a result of the resilience of membrane ion channels, neuronal spikes last twice as long as our previously reported 15 min time window. In the electrophysiological analysis, a 30 min OGD-induced dissipation of transmembrane K^+ gradient contributed differently in brain cell depolarization: severe in astrocytes and neurons, and undetectable in NG2 glia. The discrete cellular responses to OGD corresponded to a total loss of 69% of the intracellular K^+ contents in hippocampal slices as measured by Inductively Coupled Plasma Mass Spectrometry (ICP-MS). A major brain cell

*Correspondence author: Min Zhou, 4066C Graves Hall, 333 West 10th Avenue, Columbus, OH, 43210, USA; telephone: (614) 366-9406; zhou.787@osu.edu.

Conflicting interests

None.

Authors' contributions

YD and MZ: project conception and design. YD and WW: electrophysiological data collection, data analysis, and interpretation. ADL: performed the ICP-MS for K^+ measurement. BM, CMK, JWO, and ATT: discussion and assistance of the project. CCA and DMM: provision of study animals, cultured neurons, and reagents. YD, CMK, JWO, CCA, and MZ: manuscript writing. All authors corrected and approved the manuscript.

depolarization mechanism identified here is important for our understanding of cerebral ischemia pathology. Additionally, further understanding of the resilient response of NG2 glia to ischemia-induced intracellular K^+ loss and depolarization should facilitate the development of future stroke therapy.

Keywords

Astrocytes; brain ischemia; ion channel; neurons; NG2 glia

Introduction

In brain ischemia, the neuronal and glial cell depolarization appears as one of the earliest pathological events and is devastating for neuronal signaling and astrocyte homeostasis. A hypoxia-induced depolarization was initially observed in neurons and glia from *in vivo* sharp electrode recording, and the extracellular K^+ increase was indicated as the underlying mechanism[1, 2]. Later on, excessive glutamate release from various sources has been identified as an additional mechanism contributing to neuronal depolarization[3–5].

In hippocampal slices, the first sign of neuronal damage, anoxic depolarization, occurs only 7 min after oxygen-glucose deprivation (OGD) initiation with the subsequent loss of spikes in 15 min[6–8]. In contrast, astrocytes can withstand OGD for up to one hour with a fully recoverable V_M9. Neurons and glial cells differ strikingly in their ion channel expression[10] and membrane ion channels are among the first line of defense in the face of ischemic injury. It is possible that astrocytic leak-type K^+ channels and neuronal voltage-gated Na^+, Ca^{2+} and K^+ channels may exhibit different susceptibilities to ischemic insults[11, 12]. This hypothesis is plausible because the functional state of voltage-gated and leak-type K^+ channels can be either up- or down-regulated by ATP/GTP-dependent phosphorylation through various kinases in neurons and glia. Thus, these channels may respond to ischemia-induced energy failure differently[13–17]. What remains unknown is whether leak-type K^+ channels are less susceptible to ischemic insults, therefore, offering astrocytes a channel-based protective mechanism in stroke brain.

The resting V_M of a cell is established upon a physiological transmembrane K^+ gradient, 140 mM inside and 3.5 mM outside the cell, which is maintained by the Na^+-K^+-ATPase (Na^+-pump). A failure in ATP production resulting from cerebral ischemia should disable Na^+-pump activity. This, in turn, dissipates the intracellular K^+ content in a process termed K^+ gradient dissipation that results in depolarization of brain cells[18, 19]. However, the extent to which this K^+ gradient dissipation contributes to OGD-induced depolarization is unknown.

To examine how ischemic conditions acutely affect the function of ion channels and physiological ion gradients in neurons, astrocytes, and NG2 glia, we purposely used a short-term OGD paradigm to avoidlong-term ischemic conditions induced secondary injury and cell death *in situ*[11].

We show that the ion channels in neurons and glial cells are more resilient to acute OGD insults than previously anticipated. Meanwhile, the contribution of K^+ gradient dissipation to ischemia-induced membrane potential (V_M) depolarization is cell type dependent, with astrocytes and neurons severely affected and almost absent in NG2 glia. NG2 glia are progenitor cells by nature and distributed throughout the brain. Understanding of why the NG2 glia selectively resist to ischemia-induced intracellular K^+ loss and depolarization may shed lights on the novel strategy for stroke treatment in the future.

Materials and methods

Animals

All experimental procedures were approved by the Institutional Animal Care and Use Committee (IACUC) of The Ohio State University. All experimental procedures were conducted in compliance with The Ohio State University IACUC guidelines and the National Institutes of Health (NIH) Guide for the Care and Use of Laboratory Animals, 8th edition. Experiments have been reported in accordance with ARRIVE (Animal Research: Reporting of *In Vivo* Experiments) guidelines. C57BL/6N mice were used unless otherwise noted. Mice from postnatal day (P) 21–35 of both sexes weighing 9 to 16 grams were used for brain slices and freshly dissociated astrocyte preparation; P0-P1 mice were used for hippocampal neuron culture preparation. mT/mG;PDGFRα-CreER^{T2} reporter mice from P21–35 of both sexes were used for identification of NG2 glia[20].

Preparation of acute hippocampal slices

Hippocampal slices were prepared as described previously[21, 22]. Briefly, after anesthesia with 8% chloral hydrate in 0.9% NaCl, mouse brains were rapidly removed from skulls and placed into ice-cold oxygenated (95% O_2 and 5% CO_2) slice cutting artificial Cerebrospinal Fluid (aCSF) solution with reduced Ca^{2+} and increased Mg^{2+} (in mmol/L): 125 NaCl, 3.5 KCl, 25 $NaHCO_3$, 1.25 NaH_2PO_4, 0.1 $CaCl_2$, 3 $MgCl_2$ and 10 Glucose. Coronal hippocampal slices (250 μm thickness) were cut at 4°C with a Vibratome (Pelco 1500), and then transferred to a nylon-net basket in an incubator filled with oxygenated standard aCSF (in mmol/L): 125 NaCl, 25 $NaHCO_3$, 1.25 NaH_2PO_4, 3.5 KCl, 2 $CaCl_2$, 1 $MgCl_2$ and 10 Glucose (295±5 mOsm; pH 7.3–7.4) and allowed to recover at room temperature for at least one hour before recording.

Sulforhodamine (SR101) staining

For SR101 (Invitrogen) staining[23], the slices were transferred and incubated in another aCSF-filled incubator for 30 min containing 0.6 μmol/L SR101 at 34°C. Afterwards, the slices were transferred back to standard aCSF at room temperature before the experiments.

Fresh dissociation of hippocampal astrocytes

As previously described[21, 22], hippocampal slices at 250 μm thickness were sectioned from P21–35 mice. After incubation with SR101 for 30 min, the CA1 regions were dissected out, cut into small pieces (1 mm^2), and then transferred into oxygenated aCSF in a 1.5 mL microcentrifuge tube supplemented with 24U/ml papain and 0.8 mg/ml L-cysteine. This enzymatic incubation lasted for 7 min at 25°C. The loosened CA1 tissues were gently

triturated 5–7 times with a fire-polished glass pipette and then transferred into the recording chamber, where the dispersed small tissue blocks contained single to multiple gap junction-coupled astrocytes with their domains well-preserved in SR101 staining. The number of coupled astrocytes varies among these tissue blocks, which therefore offers a new model, termed the “miniature syncytium”, for the study of astrocyte membrane ion channel and gap junction coupling[21, 22, 24].

Primary hippocampal neuron cultures

Primary hippocampal neuron cultures were prepared as previously described.[25] Briefly, the hippocampus was dissected from P0-P1 mice, cut into small pieces, then transferred into Leibovitz's L-15 medium containing 0.38 mg/mL papain and 0.25 mg/mL bovine serum albumin, and then incubated at 37°C for 13 min with 95% O_2 and 5% CO_2 gas currents over the medium’s surface. After incubation, the dissected tissue was washed three times with M5-5 medium (Earle's minimal essential medium with 5% fetal bovine serum, 5% horse serum, 0.4 mmol/L L-glutamine, 16.7 mmol/L glucose, 5000 U/L penicillin, 50 mg/L streptomycin, 2.5 mg/L insulin, 16 nmol/L selenite, and 1.4 mg/L transferrin) and triturated. Dissociated cells were then centrifuged at the relative centrifugal force (RCF) of 0.048 Xg for 4.5 min, and M5-5 media was aspirated. Supplemented Neurobasal-A media was then added and the cells were resuspended (1% B27 supplement containing antioxidants, 1% B27supplement without antioxidants, 0.5 mmol/L L-glutamine, 0.5 mg/mL gentamycin, 2.5 mg/L insulin, 16 nmol/L selenite, and 1.4 mg/L transferrin). Cells were plated in 24-well cell culture plates containing 10-mm poly-D-lysine-coated glass coverslips at a density of 5×10^4 cells per well. 10 μmol/L cytosine β-d-arabinofuranoside was added 48–72 h after plating. Neurons were maintained at 37°C with 5% CO_2 for 10–14 days before experiments were performed.

Oxygen-glucose deprivation (OGD)

To simulate ischemic conditions *in situ* and *in vitro*, glucose was replaced with equimolar sucrose in aCSF, and oxygen was depleted by bubbling the solution with 95% N_2 and 5% CO_2 (pH 7.3–7.4) for 30 min prior to and throughout the 30 min OGD treatment in experiments[9].

Imaging acquisition

A fluorescent imaging system, Polychrome V system (Till Photonics, Germany) was used for high-resolution identification of SR101-positive astrocytes and eGFP-positive NG2 glia.

Measurement of intracellular K^+ contents from hippocampal slices

Inductively Coupled Plasma Mass Spectrometry (ICP-MS) was used to quantitatively measure the intracellular K^+ contents from hippocampal tissue[26, 27]. To ensure mass-equal in slices randomly distributed in the control and OGD groups, two acute hippocampal slices from the left and right hemisphere in each cut were paired as control and OGD. Slices were exposed to 30 min in either OGD conditions or normal aCSF (control). To remove the extracellular K^+, each slice was first washed with 5 mL 0.9% NaCl saline in a culture dish and then transferred into 600 μL 0.9% NaCl saline in a microcentrifuge tube. The tube was

centrifuged at RCF of 0.13 Xg for 2 min, the supernatant was discarded, and fresh 600 uL of 0.9% NaCl saline was added. This washing step was repeated three times.

For ICP-MS analysis, 0.05 mL of concentrated nitric acid (Veritas Double Distilled, GFS Chemicals Columbus, OH, USA) was added to each sample in microcentrifuge tubes. After visible signs of reaction ceased, the microcentrifuge tubes (with caps closed) were placed in a floating rack and heated to 85°C in a water bath for 30 min. After cooling, the digested samples were brought to a total volume of 0.5 mL with deionized water and then further diluted (0.1 mL aliquot of the digested solution to a final volume of 1.0 mL in 10% v/v concentrated nitric acid). The digested samples were analyzed using an ELAN 6100^{plus} DRC ICP-MS (PerkinElmer Sciex, Waltham, MA, USA) using a PFA-100 micronebulizer (Elemental Scientific, Omaha, NE, USA) at a sample uptake rate of 0.05 mL/min. K^+ was measured at m/z 39 while ammonia gas was delivered to the Dynamic Reaction Cell of the ICP-MS (with RPq=0.55, RPa=0) at a rate of 0.4 mL/min to remove the signal from $^{38}Ar^1H^+$. The K^+ content value was normalized to sample weight (μg K^+/mg sample).

Electrophysiology

A hippocampal slice was transferred to the recording chamber (RC-22, Warner Instruments, Holliston, MA) mounted on an Olympus BX51WI microscope with constant perfusion of oxygenated aCSF (2.0 mL/min). For the recording of freshly dissociated astrocytes and cultured neurons, oxygenated aCSF perfusion rate was adjusted to 1.5 mL/min.

Whole-cell patch clamp recording—MultiClamp 700A amplifier operated by pClamp 9.2 software (Molecular Devices, Sunnyvale, CA) was used for whole-cell patch clamp recording. Borosilicate glass pipettes (outer diameter: 1.5 mm, Warner Instrument, Hamden, CT) were pulled from a Micropipette Puller (Model P-87, Sutter Instrument). The recording electrodes had a resistance of 2–5 MΩ; when filled with the electrode solution containing (in mmol/L) 140 K-gluconate, 13.4 Na-gluconate, 0.5 $CaCl_2$, 1.0 $MgCl_2$, 5 EGTA, 10 HEPES, 3 Mg-ATP, and 0.3 Na-GTP (280±5 mOsm, pH 7.25–7.35) [28, 29]. A minimum of 2 GΩ; seal resistance was required before rupturing the membrane for whole-cell configuration. The liquid junction potential was compensated for prior to forming the cell-attached mode for all recordings. The V_M was recorded under current clamp mode. For neurons and NG2 glial cells, the access resistance (R_a), membrane resistance (R_M), and membrane capacitance (C_M) were measured from the “Membrane test” protocol available in pClamp 9.2 software, and only those recordings where an initial R_a below 20 MΩ; was achieved and varied less than 10% were included in data analysis. We have previously demonstrated that the “Membrane test” protocol is unable to compute the R_M and R_a from the total membrane input resistance (R_{in}) in low R_M astrocytes[30]. Thus, we alternatively used R_{in} to monitor OGD-induced change in astrocyte R_M using the “Resistance test” protocol available in PClamp 9.2 software (pulse: -63 pA/600 ms). When the initial R_{in} was greater than 20 MΩ; or varied 10% during recording, the recordings were discarded.

Cell-attached patch clamp recording—The cell-attached recording mode was used to avoid dialysis of cytoplasmic content by electrode solution[31, 32]. In this mode, the recording electrodes were filled with aCSF containing 3.5 mmol/L K^+, which reflects the extracellular

K^+ concentration ($[K^+]_e$). In recordings, the attainment of gigaohm seal was followed by a continuing negative shift in V_M toward the respective resting V_M of astrocytes, neurons, and NG2 glia, and this took 15–25 min in each recording. To ensure a constant and acceptable quality of gigaohm seal during recording, the R_{in} was monitored by "Resistance test" protocol (pulse: -63 pA/600 ms). Whenever the R_{in} fell below 1 GΩ;, an indication of deterioration of gigaohm seal, the recording was terminated and discarded.

Dual patch single astrocyte recording—As we have previously reported[21, 30, 33], two patch electrodes were targeted to an astrocytic soma. The applied positive pressure was released sequentially to form gigaohm seal in both electrodes. Negative pressure was then applied sequentially to the two electrodes to form whole-cell configuration. Both electrodes were initially set up in current clamp mode for at least 5 min for ion equilibration between the electrode solution and intracellular cytoplasm. Then one electrode was set in voltage clamp to deliver command voltages (V_{COM}), ±50 mV, and the second electrode remained in current clamp (I=0) mode. Therefore, the V_{COM} induced membrane current (ΔI_M) and voltage (ΔV_M) were simultaneously recorded by the two electrodes independently.

Data analyses

Patch clamp recording data were analyzed by Clampfit 9.0 (Molecular Devices, Sunnyvale, CA) and Origin 8.0 (OriginLab, Northampton, MA). Results are given as mean±SEM. Statistical analysis was performed using one-way ANOVA, *t*-test, and paired sample *t*-test. The significance level was set at $P<0.05$.

The $[K^+]_e$ was calculated from the Goldman-Hodgkin-Katz (GHK) equation in the following form:

$$E=(RT/F)\ln((P_K[K^+]_e+P_{Na}[Na^+]_e+P_{CI}[CI^-]_i)/(P_K[K^+]_i+P_{Na}[Na^+]_i+P_{CI}[CI^-]_e)).$$

E is the voltage across the membrane. R, T, and F are the universal gas constant, the temperature in Kelvin, and Faraday's constant, respectively. P is the relative permeability of ions at the resting V_M. $[x]_i$ and $[x]_e$ refer to the intracellular and extracellular ion concentrations, respectively. For astrocyte and NG2 glia in physiological condition, the P_K is 1, P_{Cl} is assumed at 0 and P_{Na} is 0.015[34]. For neurons in the resting condition, the P_K is 1.0, and P_{Cl} and P_{Na} are assumed at 0.45 and 0.05, respectively [35]. Astrocyte membrane conductance (G_M) was calculated from the following equation:

$$G_M=\Delta I_M/\Delta V_M$$

ΔV_M and ΔI_M were V_{COM} induced change in V_M and I from dual patch single cell recording. The G_M in inward and outward directions was calculated from the $\Delta I_M/\Delta V_M$ induced by the V_{COM} of -50 mV and +50 mV, respectively.

A question we asked was the OGD impact on voltage-gated inward Na^+ currents (INa), outward transient (IKa) and delayed rectifying (IKd) in both neurons and NG2 glia. In these electrophysiological analyses, we did not isolate individual channel components through

channel pharmacology to examine the effect of OGD on channel activation/inactivation kinetics for the following considerations[36, 37]. First, the purpose of this study was to examine the overall impact of OGD on neuronal and glial voltage-gated ion channels, rather than the OGD effect on a given type of ion channel. Second, the pharmacological blockers may influence the activity of the investigated channel through additional pathways. Finally, it is not feasible to maintain a viable recording in OGD with the addition of multiple blockers that typically lasts for 70–90 min. For the purpose of following electrophysiology conventions, we still used *I*Na, *I*Ka, and *I*Kd in general terms for the following description.

Results

Electrophysiological responses of astrocytes, NG2 glia, and pyramidal neurons to OGD

To examine the electrophysiological response of astrocytes to 30 min OGD insults, astrocytes in hippocampal CA1 *stratum radiatum* were identified based on their SR101 positive staining (Figure 1(a)). Recorded astrocytes showed a resting V_M of -76.9±0.70 mV (n=14), and a characteristic passive membrane conductance (Figure 1(d))[21, 38]. As we reported previously[9], astrocyte's V_M progressively depolarized during OGD that amounted to 12.3±1.72 mV (n=14) in the end of the 30 min treatment. OGD withdrawal was followed by a rapid return of the V_M to the resting baseline, and a subsequent hyperpolarization (-5.7±0.70 mV, n=14), resulting from OGD-induced over activation of Na^+/K^+-ATPase (Figure 1(g))[9, 38].

It is still unknown how NG2 glia, another subtype of glia in the brain, responds to OGD. NG2 glia are morphologically similar to astrocytes, yet devoid of SR101 staining and gap junctional coupling (Figure 1(b)) [39]. In some experiments, NG2 glia were directly identified from mT/mG;PDGFRα-CreER^{T2} reporter mice as we previously reported[22]. The NG2 glia characteristically express a small voltage-gated Na^+ (*I*Na), outward transient (*I*Ka) and delayed rectifier (*I*Kd) K^+ conductance in addition to inward rectifying $K_{ir}4.1$ K^+ conductance(Figure 1(e))[36, 40–42]. NG2 glia exhibited a resting V_M of -78.0±0.56 mV (n=23). During the 30 min OGD exposure, the peak V_M depolarization occurred earlier at 19.3±0.93 min and amounted to 9.2±1.57 mV. OGD withdrawal was followed by a hyperpolarization, -4.15±1.52 mV (Figure 1(h), n=12).

To examine how CA1 pyramidal neurons respond to OGD, these neurons were identified for recording based on their location and characteristic somatic shape (Figure 1(c)). As we previously reported[6, 7, 43], a large inward *I*Na, outward *I*Ka and *I*Kd could be sequentially activated by depolarization steps (Figure 1(f), top). Pyramidal neurons exhibited a resting V_M of -62.9±0.71 mV (n=17), absent of spontaneous firing at rest, and adaptation in firing spikes in response to current injection (Figure 1(f), bottom). A 30 min OGD induced consistent electrophysiological changes in pyramidal neurons. Specifically, there was an initial increase and then total loss of firing spikes. In 71% of the recorded neurons (12/17) the V_M depolarization amounted to 9.8±2.24 mV with an >80% of recovery following aCSF washout (Figure 1(i)). In another 29% of neurons (5/17), the post-OGD V_M recovery in washout did not reach to 80%. This most likely reflects a more severe OGD damage and this group of neurons was not included in data analysis.

The intrinsic properties of astrocyte leak K^+ channels remain intact during OGD

In contrast to excitable neurons, astrocytes predominantly express leak-type K^+ channels[44]. While OGD-induced dysfunction of leak K^+ channels should contribute to astrocyte depolarization, evidence in support of this notion remains unavailable. We began to test this idea using freshly dissociated single be well-preserved in these process-bearing single native astrocytes (Figure 2(a))[21, 22]. Second, only in this uncoupled state can the intracellular K^+ concentration ($[K^+]_i$) of astrocyte be concentration-clamped by the recording electrode[36, 45]. Finally, the $[K^+]_e$ can be controlled at the level of aCSF perfusion (Figure 2(b)). These factors together create a constant transmembrane K^+ gradient so that any OGD-induced damage to astrocyte K^+ channels can be unequivocally revealed as V_M depolarization or a decrease in G_M.

In our first experiment, the recorded single astrocytes in control conditions showed a comparable resting V_M as astrocytes *in situ*. This V_M remained unchanged during OGD exposure and the following washout in aCSF (Figure 2(c) and (d), $P>0.05$). To ensure the quality of these long-lasting recordings, the input resistance (R_{in}) was monitored throughout the experiment (Figure 2(e), $P>0.05$). These results indicate that OGD exerted no detectable damage to astrocyte K^+ channels.

In the second experiment, dual patch single astrocyte recording in slices was used to further explore any OGD-induced change in astrocyte G_M (Figure 2(f)). Although technically demanding, this is currently the only methodology allowing accurate analysis of G_M from low membrane resistance astrocytes (R_M=5.6 MΩ;)[21, 30, 33]. In line with the unchanged V_M above, a 30 min OGD exerted no detectable decrease in astrocyte G_M in both inward and outward directions (Figure 2(g) and (h)). This further confirms that a short-term OGD exposure does not impose a measurable change in astrocyte leak K^+ channels function.

The intrinsic properties of NG2 glia K^+ channels remain intact during OGD

Although both astrocytes and NG2 glia express $K_{ir}4.1$ (I_{Kir}), NG2 glia also express voltage-gated I_{Ka} and I_{Kd} K^+ conductances. How these neuronal K^+ channels respond to OGD is unknown. Interestingly, a 30 min OGD exposure did not change NG2 glia I_{Kir}, IKa, and IKd (Figure 2(i)–(m)). Specifically, the current profiles (Figure 2(i) and (j)),and the current amplitudes in I-V plots (Figure 2(k) (l) (m)) remained unaltered in OGD (n=4, $P>0.05$, paired sample t-test). Thus, the acute OGD insults also exert a negligible impact on the glial type voltage-gated K^+ conductances. Because of the low density and heterogeneous INa expression, we did not quantitatively analyze the OGD effect on NG2 glia INa[36].

Neuronal leak K^+ channels remain functional during OGD

To answer whether neuronal ion channels would be more susceptible to a short-term OGD insult, cultured hippocampal neurons were used for the following considerations. First, only in this pure neuronal culture preparation, can the direct OGD imposed damage to neuronal ion channels be unequivocally identified. Second, cultured neurons exhibit nearly identical electrophysiological features as neurons in slices (Figure 3(a) and (b)). Specifically, cultured neurons exhibited a resting V_M of -61.8±1.38 mV (n=24), and expression of voltage-gated Na^+ and K^+ channels that are comparable to hippocampal neurons *in situ*. Third, although

freshly dissociated hippocampal neurons would be a suitable preparation for this study, isolated neurons have low viability to withstand a long-lasting whole-cell recording.

In 43% (10/23) of recorded neurons, OGD induced only a slight but fully recoverable V_M depolarization of 2.1±0.87 mV. This depolarization was significantly less than neurons in brain slice (9.7±2.64 mV, Figure 3(c) and (d), $P<0.01$). In the remaining 57 % (13/23) of neurons, depolarization was not detectable during a 30 min OGD and in the following washout (Figure. 3(c) and (e), $P>0.05$). These results indicated that the functional leak K^+ channels that establish the neuronal resting V_M are insensitive to OGD insults.

Neuronal voltage-gated Na^+ and K^+ channels remain intact over a 30 min OGD

Neuronal voltage-gated Na^+ and K^+ channels work in concert to generate action potentials. To determine whether this category of neuronal ion channels would be more susceptible to OGD insults, we first examined the OGD impact on spontaneous firing in cultured hippocampal neurons. Consistent with the co-existence of diverse neuronal types in this preparation, neuronal responses to OGD fell into three different patterns (Figure 3(c)): 1) spontaneous firing in control, then an initial increase in firing with a subsequent decrease in firing during OGD; 2) spontaneous firing in control, diminished firing in OGD; 3) no spontaneous firing throughout the recording. To determine whether OGD affects neuronal firing, action potentials were induced by current injections (Figure 3(f)–(i)) for comparison of changes in neuronal firing frequency and amplitude. OGD induced no changes in these neuronal firing parameters over a 30 min treatment (Figure 3(j) and (k), $P>0.05$).

We next examined the direct impact of OGD on the function of voltage-gated ion channels. First, we examined the current density of INa, IKa, and IKd in voltage clamp recording[46]. Surprisingly, the neuronal INa could still be fully activated with no change in current density after 30 min in OGD (V_{COM} at -40 to -30 mV). Also, there was no change in the current densities of either IKa or IKd (V_{COM} of +40 mV, $P>0.05$) (Figure 4(a)–(c)). The current amplitudes of INa, IKa, and IKd at each voltage steps were comparable in control and 30 min OGD (Figure 4(d)–(f)). Together, neuronal voltage-gated Na^+ and K^+ channels are highly resistant to a short-term OGD.

K^+ gradient dissipation contributes significantly to OGD-induced astrocyte depolarization

Energy failure is known to dissipate the intracellular K^+ content that in turn depolarizes the cell. However, it remains technically challenging to determine its relative contribution to OGD-induced brain cell depolarization because $[K^+]_i$ loss is compensated by the electrode K^+ in whole-cell recording (Figure 2(b)).

Here we considered the use of freshly dissociated hippocampal tissues as a unique model to address this question, where each tissue contains a variable number of gap junction-coupled astrocytes or “miniature syncytium” [22]. We have previously shown that the recorded astrocyte in a miniature syncytium is readily concentration-clamped by the electrode solution to maintain a physiological V_M. However, due to a strong electrical coupling, the recorded V_M is the aggregate V_M of the entire network[22]. Thus, the OGD-induced K^+ gradient dissipation and its resultant depolarization in the neighboring astrocytes should

offset the physiological V_M in the recorded astrocyte, and the degree of V_M offset is proportional to the number of astrocytes in a syncytium[22].

As predicted, a syncytium size-dependent V_M depolarization was observed. Specifically, with more astrocytes present in a miniature syncytium, the greater OGD-induced depolarization became (Figure 5(a) and (b)). In a miniature syncytium containing 3–7 astrocytes, OGD-induced peak V_M depolarization was 5.4±0.57 mV. In a syncytium containing >10 astrocytes, the recorded astrocyte depolarized by 12.9±1.28 mV, which was comparable to astrocyte depolarization observed in brain slices (Figure 5(c)).

In this experiment, we also compared and analyzed the passive conductance from the following groups: 1) astrocytes *in situ* and in miniature syncytia with greater than 10 astrocytes, and 2) single astrocytes and astrocytes in miniature syncytia with less than 3 astrocytes. A 30 min OGD exerted no change in passive conductance (Figure 5(d)–(f)). These findings corroborate the conclusion in Figure 2 that the intrinsic properties of astrocyte K^+ channels are not altered in OGD.

Altogether, contrary to a prevailing view that astrocyte depolarization is proportional to the increase in $[K^+]_e$, our results argue that astrocyte depolarization is mainly an indicator of the severity of $[K^+]_i$ gradient dissipation in the stroke brain.

The actual OGD-induced depolarization and $[K^+]_i$ loss in CNS cells

To better understand the extent of $[K^+]_i$ loss during OGD, it is critical to know the actual OGD-induced depolarization in astrocytes, neurons, and NG2 glia. To circumvent the problematic ion dialysis in conventional whole-cell recording, cell-attached patch clamp mode was used in the following experiments. In this recording mode, the ion exchange between electrode and cytoplasm can be minimized[31, 32].

The difference between conventional and cell-attached recording configuration is schematically illustrated for astrocyte recording (Figure 6(a)), and successful prevention of ion dialysis was demonstrated (Figure 6(b). During cell-attached recording, the gigaohm seal formation was followed by a gradual V_M hyperpolarization to the anticipated resting V_M of -75.8±1.04 mV in 15–20 min, which was comparable to the astrocyte V_M recorded from whole-cell mode (Figure 6(c) and (d), left; (e), $P>0.05$). Similar to the whole-cell recording, a 30 min OGD-induced depolarization was fully reversible (Figure 6(d)). Surprisingly, the OGD- induced depolarization (41.5±3.15 mV, n=8) was 3-folds greater than that of the conventional whole-cell recording (Figure 6(c) and (d), right; (f), $P<0.01$).

In NG2 glia cell-attached recording, the recorded V_M also gradually hyperpolarized to the resting V_M of -77.8±1.02 mV ($n=13$) in 15–20 min (Figure 6(g), left), which was comparable to the V_M recorded from the whole-cell mode (-78.0±0.56 mV, $n=23$). Interestingly, the OGD-induced NG2 glia depolarization (8.7±2.41 mV, $n=7$) did not differ from the depolarization measured from conventional whole-cell mode (9.2±1.57 mV, $n=12$) (Figure 6(g), right; and (h), $P>0.05$). Unlike astrocytes, NG2 glia are not gap junction coupled with each other or with other types of brain cells. Thus, a similar level of depolarization observed in these two recording modes indicates a negligible loss of

intracellular K^+ content during OGD. Further, this conclusion suggests that OGD-induced depolarization in NG2 glia most likely reflects the dynamic increase in $[K^+]_e$ during OGD.

In cell-attached recording from hippocampal pyramidal neurons *in situ*, the recorded V_M gradually hyperpolarized to the resting V_M of -60.0±0.92 mV in 20–30 min after gigaohm seal, which was also comparable to the V_M recorded from whole-cell mode (Figure 7(a) and (d)). However, the OGD-induced depolarization was significantly greater than conventional whole-cell recording and the majority of neurons suffered from more severe damage. Specifically, only 26% (5/19) of neurons survived through a 30 min OGD with a fully reversible V_M. The depolarization in this group of neurons amounted to 55.1±1.39 mV, which was 6-folds greater than in whole-cell recording (Figure 7(b) and (e), $P<0.01$). The depolarization in the remaining 74% (14/19) of neurons was greater, 70.3±1.87 mV, and could only be partially recovered in washout (Figure 7(c) and (e)). We have previously shown that extension of OGD from 15 min to 20 min results in a 2.4-fold increase in neuronal death[7], which explains why a large percentage of neurons could not achieve a full functional recovery after a 30 min OGD treatment. It should be noted that for those recordings with a full V_M recovery, neuronal firing re-emerged in aCSF washout (Figure 7(b)), reinforcing the notion that the neuronal voltage-gated ion channels are highly resistant to short-term ischemic insults.

In summary, under the condition that the change in OGD-induced intracellular K^+ content was not disturbed in cell-attached recording, a considerably high level of V_M depolarization was revealed from astrocytes and neurons, but not NG2 glia. Therefore, K^+ gradient dissipation should be a major contributor to OGD-induced depolarization in astrocytes and neurons.

OGD-induced loss of intracellular K^+ contents in hippocampal slices

ICP-MS measurements were made to definitively assess K^+ gradient dissipation in response to OGD and to quantify the change in intracellular K^+ content. The ICP-MS measurements showed that after 30 min of OGD, there was a significant reduction of K^+ in hippocampal slices: 2.7±0.23 μg/mg in control vs. 0.8±0.24 μg/mg in OGD ($n=6$, $P<0.01$, *t*-test). These results represent a 69% loss of intracellular K^+ in slices.

ICP-MS theoretically provides the sensitivity for detection of a trace amount of K^+ content from a single cell. Therefore, a further attempt was made to correlate the above observation to freshly dissociated single neurons and astrocytes. However, a rather small single cell vs. medium volume ratio in collected single cell samples did not allow reliable separation of K^+ content in a single cell from the K^+ in the sample medium. Thus, we could not proceed further to gain specific cell type information in the present study.

Yet the results in slices support the conclusion drawn from the electrophysiological experiments. Together, these experiments indicate that the dissipation in the K^+ gradient in cells following OGD exposure is robust and strongly suggest that K^+ gradient dissipation is a major contributor to ischemia-induced depolarization in neurons and astrocytes.

Discussion

Among various pathological events that could contribute either directly or indirectly to ischemia-induced V_M depolarization, excessive $[K^+]_e$ and $[Glut]_e$ have been well-characterized[3, 4, 18, 19, 47]. A failure in ion channel function is also known to disrupt the membrane potential and neuronal activity. However, its relative contribution to ischemic pathology is poorly defined. In the present study, we show that ion channels in both excitable neurons and electrically silent astrocytes and NG2 glia are highly resistant to OGD insults. We also show, for the first time, that the dissipation of the physiological K^+ gradient contributes significantly to ischemia-induced depolarization in astrocytes and neurons, but not NG2 glia.

Membrane ion channels in glial cells and neurons are resilient to short-term ischemic insults

OGD has been shown to depolarize syncytial coupled astrocytes *in situ* (Figure 1)[9, 48, 49]. An important clarification made in this study is that the depolarization is not caused by direct OGD impairment of astrocyte leak K^+ channels. This idea is supported by several experiments. Using single freshly dissociated astrocytes to eliminate the depolarization resulting from K^+ gradient dissipation, an additional depolarization resulting from a direct OGD impairment of K^+ channels was not observed (Figure 2). Further, the characteristic passive conductance of the cell membrane, which results from a complex expression of multiple known and unknown K^+ channels, was not altered by OGD (Figure 5) [21, 24, 38, 44]. Finally, a 30 min OGD exposure imposed no detectable change in astrocyte membrane leak K^+ conductance (G_M) *in situ* (Figure 2). This indicates that the intrinsic properties of K^+ channels remain unchanged even when exposed to a more severe pathological environment initiated by OGD, which includes acidosis and an excessive glutamate and GABA in brain slices. This resiliency in astrocyte K^+ channels should serve as a channel-based mechanism allowing astrocytes to function continuously during brain ischemia[9].

In the present study, we also examined the ion channel responses of NG2 glia to OGD. NG2 glia express several voltage-gated K^+ channels in addition to $K_{ir}4.1$. In line with the observation from astrocytes, the I_{Kir} was not altered by OGD. Additionally, the glial type of voltage-gated I_{Ka} and I_{Kd} in NG2 glia was not affected by a short-term OGD (Figure 2).

Another important observation made in this study is that neuronal leak K^+ channels, as well as voltage-gated ion channels, are highly resistant to OGD insults (Figure 3 and 4). Thus, a rapid loss of neuronal excitability in OGD is not attributable to the direct impairment of the neuronal ion channels themselves.

Ischemia-induced K^+ gradient dissipation contributes differently to NG2 glial, astrocytic, and neuronal depolarization

Under the condition that the pathological change in $[K^+]_i$ was not disturbed by ion dialysis in cell-attached recording mode, the OGD-induced NG2 glia depolarization did not differ from what was recorded from the conventional whole-cell recording. This strongly indicates that the $[K^+]_i$ in single uncoupled NG2 glia was maintained at a physiological level, or the

OGD-induced loss of $[K^+]_i$ was minimal. Similar to astrocytes, NG2 glia predominantly express K^+ channels and it has been shown that the high-density expression of $K_{ir}4.1$ enables NG2 glia to behave as K^+ electrodes[42]. Therefore, the recorded NG2 glia V_M should to mainly reflect the dynamic change of $[K^+]_e$ in OGD (Figure 1(h)). According to the GHK equation, the peak NG2 glia depolarization corresponds to a $[K^+]_e$ of 6.08 mmol/L in OGD.

In contrast to NG2 glia, the cell-attached astrocyte recording revealed an OGD-induced depolarization of 41.5 mV. This was 3 folds greater than whole-cell recording. We have previously shown that OGD-induced activation of astrocytic ionotropic receptors, transporters, and exchangers has a negligible contribution to OGD-induced depolarization in hippocampal astrocytes[9]. Astrocytes exhibit very low or absent Na^+, Cl^- and Ca^{2+} permeabilities at resting conditions[29, 34]. Here we further show that OGD impairment to astrocyte K^+ channels is barely detectable (Figure 2). By elimination, the K^+ gradient dissipation appears to be a major cause of astrocyte depolarization in the early phase of ischemic brain injury. Considering an OGD-induced peak value of $[K^+]_e$ at 6.08 mmol/L as discussed above from NG2 glia, a 41.5 mV depolarization indicates a dissipation of $[K^+]_i$ in astrocytes from the physiological 140 mmol/L to 39 mmol/L, or a total loss of 101 mmol/L, at the end of 30 min of OGD.

In hippocampal pyramidal neurons *in situ*, OGD-induced V_M depolarization was 6-fold greater in cell-attached mode than in conventional whole-cell mode (Figure 7), and this was accompanied by a significantly high number of neurons suffering from irreversible OGD damage to their V_M. This indicates that a severe OGD-induced $[K^+]_i$ dissipation should also occur in neurons. However, neuronal depolarization is known to be involved in multiple complex events, such as activation of various ionotropic receptors and transporters. These events should be associated with dynamic changes in the permeabilities of K^+ relative to Na^+, Ca^{2+}, and Cl^- [35]. Additionally, neuronal ATP sensitive K^+ channels (K_{ATP}) are activated in OGD conditions[50], and this should partially offset the actual depolarization, especially in cell-attached mode where the recorded V_M represented more of the K_{ATP}-enriched neuronal soma. Because of the complexity of brain ischemia, the exact contribution of K^+ gradient dissipation to OGD-induced neuronal depolarization could not be quantitatively defined in this study. Thus, more research would be needed in the future to dissect out the individual contribution of these factors to the overall OGD-induced depolarization in neurons.

Finally, we used ICP-MS to directly assess the OGD-induced loss of intracellular K^+. The results revealed that in hippocampal slices containing a variety of cell types, a 30 min OGD induced a 69% loss of K^+ content. Considering that astrocytes and neurons occupy most of the brain volume, the resultant intracellular K^+ loss is largely in line with our electrophysiological analysis in OGD.

Regeneration of CNS cells from survival NG2 glia in stroke brain?

While K^+ gradient dissipation has been uncovered as a major cause underlying astrocytic and neuronal depolarization in ischemia, an important aspect emerging from the present study lies in the discrete cellular responses to OGD in terms of the loss in the intracellular K^+ content. Only NG2 glia, also termed oligodendrocyte precursor cells (OPCs), are selectively and highly resistant to the loss of intracellular K^+ gradient in OGD. Other than

being a precursor in oligodendrocyte lineage, NG2 glia constitutes ~5% of brain cells and are distributed throughout the brain[51–53]. The majority of these glial cells are mitotically quiescent throughout the life with no clearly defined role in brain function[51].

A number of physiological features may account for the remarkable ability of NG2 glia in maintaining the physiological ion gradients in stroke brain. As a non-excitable glial subtype in the brain, NG2 glia do not fire action potentials, a physiological process of high energy consuming, and express low density of leak type K^+ channels compared with astrocytes for K^+ efflux in ischemic conditions. Recent gene profiling study indicates significantly higher levels of expression of Na^+-K^+ ATPase α1 subunit in NG2 glia when compared to astrocytes and neurons[54, 55]. Although we still know little about how NG2 glia access to energy substrate and whether they switch to using glycolysis for ATP production, such a high-level expression of α1 subunit may be an important player in maintaining the physiological K^+ gradient in the presence of ATPs. Additionally, NG2 glia are able to rapidly proliferating and migrating to sites of focal injury[56]. In different culture conditions, increasing evidence points to the multipotential of NG2 glia to give rise to not only oligodendrocytes but also astrocytes and neurons[57–59]. In the present study, only NG2 glia exhibit the ability to retain their physiological K^+ gradient, therefore, continuing functioning in the acute phase of ischemic brain. These findings further support a recent proposal that NG2 glia are a promising target for the development of novel therapies for stroke treatment[60].

Conclusion

In summary, the membrane ion channels in hippocampal neurons and glial cells can withstand OGD over an extended time period, therefore, contribute minimally to OGD-induced depolarization. In contrast, K^+ gradient dissipation contributes significantly to CNS cell depolarization in cerebral ischemia.

Acknowledgments

Sources of Funding

This work is sponsored by grants from National Institute of Neurological Disorders and Stroke RO1NS062784, R56NS097972 (MZ), RO1NS082095 (DMM), and American Heart Association Award 16GRNT31340002 (CCA).

References

1. Muller M, Somjen GG. Na(+) and K(+) concentrations, extra- and intracellular voltages, and the effect of TTX in hypoxic rat hippocampal slices. Journal of neurophysiology. 2000; 83:735–45. [PubMed: 10669489]
2. Leblond J, Krnjevic K. Hypoxic changes in hippocampal neurons. Journal of neurophysiology. 1989; 62:1–14. [PubMed: 2547034]
3. Kimelberg HK, Goderie SK, Higman S, Pang S, Waniewski RA. Swelling-induced release of glutamate, aspartate, and taurine from astrocyte cultures. J Neurosci. 1990; 10:1583–91. [PubMed: 1970603]
4. Rossi DJ, Oshima T, Attwell D. Glutamate release in severe brain ischaemia is mainly by reversed uptake. Nature. 2000; 403:316–21. [PubMed: 10659851]
5. Fleidervish IA, Gebhardt C, Astman N, Gutnick MJ, Heinemann U. Enhanced spontaneous transmitter release is the earliest consequence of neocortical hypoxia that can explain the disruption of normal circuit function. J Neurosci. 2001; 21:4600–8. [PubMed: 11425888]

6. Zhang H, Xie M, Schools GP, et al. Tamoxifen mediated estrogen receptor activation protects against early impairment of hippocampal neuron excitability in an oxygen/glucose deprivation brain slice ischemia model. Brain Res. 2009; 1247:196–211. [PubMed: 18992727]
7. Zhang H, Schools GP, Lei T, Wang W, Kimelberg HK, Zhou M. Resveratrol attenuates early pyramidal neuron excitability impairment and death in acute rat hippocampal slices caused by oxygen-glucose deprivation. Exp Neurol. 2008; 212:44–52. [PubMed: 18495119]
8. Allen NJ, Karadottir R, Attwell D. A preferential role for glycolysis in preventing the anoxic depolarization of rat hippocampal area CA1 pyramidal cells. J Neurosci. 2005; 25:848–59. [PubMed: 15673665]
9. Xie M, Wang W, Kimelberg HK, Zhou M. Oxygen and glucose deprivation-induced changes in astrocyte membrane potential and their underlying mechanisms in acute rat hippocampal slices. Journal of cerebral blood flow and metabolism : official journal of the International Society of Cerebral Blood Flow and Metabolism. 2008; 28:456–67.
10. Cahoy JD, Emery B, Kaushal A, et al. A transcriptome database for astrocytes, neurons, and oligodendrocytes: a new resource for understanding brain development and function. The Journal of neuroscience : the official journal of the Society for Neuroscience. 2008; 28:264–78. [PubMed: 18171944]
11. Rossi DJ, Brady JD, Mohr C. Astrocyte metabolism and signaling during brain ischemia. Nat Neurosci. 2007; 10:1377–86. [PubMed: 17965658]
12. Martin RL, Lloyd HG, Cowan AI. The early events of oxygen and glucose deprivation: setting the scene for neuronal death? Trends in neurosciences. 1994; 17:251–7. [PubMed: 7521086]
13. Scheuer T. Regulation of sodium channel activity by phosphorylation. Seminars in cell & developmental biology. 2011; 22:160–5. [PubMed: 20950703]
14. Maier LS. CaMKII regulation of voltage-gated sodium channels and cell excitability. Heart rhythm : the official journal of the Heart Rhythm Society. 2011; 8:474–7.
15. Shah NH, Aizenman E. Voltage-gated potassium channels at the crossroads of neuronal function, ischemic tolerance, and neurodegeneration. Translational stroke research. 2014; 5:38–58. [PubMed: 24323720]
16. Vacher H, Trimmer JS. Diverse roles for auxiliary subunits in phosphorylation-dependent regulation of mammalian brain voltage-gated potassium channels. Pflugers Arch. 2011; 462:631–43. [PubMed: 21822597]
17. Rojas A, Cui N, Su J, Yang L, Muhumuza JP, Jiang C. Protein kinase C dependent inhibition of the heteromeric Kir4.1-Kir5.1 channel. Biochim Biophys Acta. 2007; 1768:2030–42. [PubMed: 17585871]
18. Hansen AJ. Effect of anoxia on ion distribution in the brain. Physiol Rev. 1985; 65:101–48. [PubMed: 3880896]
19. Rothman SM, Olney JW. Glutamate and the pathophysiology of hypoxic--ischemic brain damage. Annals of neurology. 1986; 19:105–11. [PubMed: 2421636]
20. Hesp ZC, Goldstein EZ, Miranda CJ, Kaspar BK, McTigue DM. Chronic oligodendrogenesis and remyelination after spinal cord injury in mice and rats. J Neurosci. 2015; 35:1274–90. [PubMed: 25609641]
21. Du Y, Ma B, Kiyoshi CM, Alford CC, Wang W, Zhou M. Freshly dissociated mature hippocampal astrocytes exhibit passive membrane conductance and low membrane resistance similarly to syncytial coupled astrocytes. J Neurophysiol. 2015; 113:3744–50. [PubMed: 25810481]
22. Ma B, Buckalew R, Du Y, et al. Gap junction coupling confers isopotentiality on astrocyte syncytium. Glia. 2016; 64:214–26. [PubMed: 26435164]
23. Nimmerjahn A, Kirchhoff F, Kerr JN, Helmchen F. Sulforhodamine 101 as a specific marker of astroglia in the neocortex in vivo. Nat Methods. 2004; 1:31–7. [PubMed: 15782150]
24. Zhong S, Du Y, Kiyoshi CM, et al. Electrophysiological behavior of neonatal astrocytes in hippocampal stratum radiatum. Molecular brain. 2016; 9:34. [PubMed: 27004553]
25. Sherwood TW, Lee KG, Gormley MG, Askwith CC. Heteromeric acid-sensing ion channels (ASICs) composed of ASIC2b and ASIC1a display novel channel properties and contribute to acidosis-induced neuronal death. The Journal of neuroscience : the official journal of the Society for Neuroscience. 2011; 31:9723–34. [PubMed: 21715637]

26. Wald T, Petry-Podgorska I, Fiser R, et al. Quantification of potassium levels in cells treated with Bordetella adenylate cyclase toxin. Analytical biochemistry. 2014; 450:57–62. [PubMed: 24412166]
27. Lin VJT, Zolekar A, Shi Y, et al. Potassium as a pluripotency-associated element identified through inorganic element profiling in human pluripotent stem cells. Scientific reports. 2017:7. [PubMed: 28127057]
28. Kelly T, Kafitz KW, Roderigo C, Rose CR. Ammonium-evoked alterations in intracellular sodium and pH reduce glial glutamate transport activity. Glia. 2009; 57:921–34. [PubMed: 19053055]
29. Ma BF, Xie MJ, Zhou M. Bicarbonate efflux via GABA(A) receptors depolarizes membrane potential and inhibits two-pore domain potassium channels of astrocytes in rat hippocampal slices. Glia. 2012; 60:1761–72. [PubMed: 22855415]
30. Ma B, Xu G, Wang W, Enyeart JJ, Zhou M. Dual patch voltage clamp study of low membrane resistance astrocytes in situ. Mol Brain. 2014; 7:18. [PubMed: 24636341]
31. Mason MJ, Simpson AK, Mahaut-Smith MP, Robinson HP. The interpretation of current-clamp recordings in the cell-attached patch-clamp configuration. Biophysical journal. 2005; 88:739–50. [PubMed: 15516522]
32. Perkins KL. Cell-attached voltage-clamp and current-clamp recording and stimulation techniques in brain slices. J Neurosci Methods. 2006; 154:1–18. [PubMed: 16554092]
33. Zhou M, Xu G, Xie M, et al. TWIK-1 and TREK-1 are potassium channels contributing significantly to astrocyte passive conductance in rat hippocampal slices. The Journal of neuroscience : the official journal of the Society for Neuroscience. 2009; 29:8551–64. [PubMed: 19571146]
34. Langer J, Stephan J, Theis M, Rose CR. Gap junctions mediate intercellular spread of sodium between hippocampal astrocytes in situ. Glia. 2012; 60:239–52. [PubMed: 22025386]
35. Hille, B. Ion channels of excitable cells. Sunderland, MA: Sinauer; 2001.
36. Xie M, Lynch DT, Schools GP, Feustel PJ, Kimelberg HK, Zhou M. Sodium channel currents in rat hippocampal NG2 glia: characterization and contribution to resting membrane potential. Neuroscience. 2007; 150:853–62. [PubMed: 17981402]
37. Zhou M, Kimelberg HK. Freshly isolated astrocytes from rat hippocampus show two distinct current patterns and different [K(+)](o) uptake capabilities. J Neurophysiol. 2000; 84:2746–57. [PubMed: 11110805]
38. Wang W, Kiyoshi CM, Du Y, et al. mGluR3 Activation Recruits Cytoplasmic TWIK-1 Channels to Membrane that Enhances Ammonium Uptake in Hippocampal Astrocytes. Mol Neurobiol. 2015
39. Zhou M, Schools GP, Kimelberg HK. Development of GLAST(+) astrocytes and NG2(+) glia in rat hippocampus CA1: mature astrocytes are electrophysiologically passive. J Neurophysiol. 2006; 95:134–43. [PubMed: 16093329]
40. Steinhauser C, Berger T, Frotscher M, Kettenmann H. Heterogeneity in the Membrane Current Pattern of Identified Glial Cells in the Hippocampal Slice. Eur J Neurosci. 1992; 4:472–84. [PubMed: 12106333]
41. De Biase LM, Nishiyama A, Bergles DE. Excitability and synaptic communication within the oligodendrocyte lineage. The Journal of neuroscience : the official journal of the Society for Neuroscience. 2010; 30:3600–11. [PubMed: 20219994]
42. Maldonado PP, Velez-Fort M, Levavasseur F, Angulo MC. Oligodendrocyte precursor cells are accurate sensors of local k+ in mature gray matter. The Journal of neuroscience : the official journal of the Society for Neuroscience. 2013; 33:2432–42. [PubMed: 23392672]
43. Zhang H, Cao HJ, Kimelberg HK, Zhou M. Volume regulated anion channel currents of rat hippocampal neurons and their contribution to oxygen-and-glucose deprivation induced neuronal death. PLoS One. 2011; 6:e16803. [PubMed: 21347298]
44. Olsen ML, Khakh BS, Skatchkov SN, Zhou M, Lee CJ, Rouach N. New Insights on Astrocyte Ion Channels: Critical for Homeostasis and Neuron-Glia Signaling. J Neurosci. 2015; 35:13827–35. [PubMed: 26468182]
45. Bergles DE, Roberts JD, Somogyi P, Jahr CE. Glutamatergic synapses on oligodendrocyte precursor cells in the hippocampus. Nature. 2000; 405:187–91. [PubMed: 10821275]

46. Tombaugh GC, Somjen GG. Effects of extracellular pH on voltage-gated Na+, K+ and Ca2+ currents in isolated rat CA1 neurons. The Journal of physiology. 1996; 493(Pt 3):719–32. [PubMed: 8799894]
47. Leis JA, Bekar LK, Walz W. Potassium homeostasis in the ischemic brain. Glia. 2005; 50:407–16. [PubMed: 15846795]
48. Xu G, Wang W, Kimelberg HK, Zhou M. Electrical coupling of astrocytes in rat hippocampal slices under physiological and simulated ischemic conditions. Glia. 2010; 58:481–93. [PubMed: 19795502]
49. Pivonkova H, Benesova J, Butenko O, Chvatal A, Anderova M. Impact of global cerebral ischemia on K+ channel expression and membrane properties of glial cells in the rat hippocampus. Neurochem Int. 2010; 57:783–94. [PubMed: 20833221]
50. Huang CW, Huang CC, Cheng JT, Tsai JJ, Wu SN. Glucose and hippocampal neuronal excitability: role of ATP-sensitive potassium channels. J Neurosci Res. 2007; 85:1468–77. [PubMed: 17410601]
51. Nishiyama A, Watanabe M, Yang Z, Bu J. Identity, distribution, and development of polydendrocytes: NG2-expressing glial cells. J Neurocytol. 2002; 31:437–55. [PubMed: 14501215]
52. Dawson MR, Polito A, Levine JM, Reynolds R. NG2-expressing glial progenitor cells: an abundant and widespread population of cycling cells in the adult rat CNS. Mol Cell Neurosci. 2003; 24:476–88. [PubMed: 14572468]
53. Nishiyama A, Komitova M, Suzuki R, Zhu X. Polydendrocytes (NG2 cells): multifunctional cells with lineage plasticity. Nat Rev Neurosci. 2009; 10:9–22. [PubMed: 19096367]
54. Zhang Y, Sloan SA, Clarke LE, et al. Purification and Characterization of Progenitor and Mature Human Astrocytes Reveals Transcriptional and Functional Differences with Mouse. Neuron. 2016; 89:37–53. [PubMed: 26687838]
55. Zhang Y, Chen K, Sloan SA, et al. An RNA-sequencing transcriptome and splicing database of glia, neurons, and vascular cells of the cerebral cortex. J Neurosci. 2014; 34:11929–47. [PubMed: 25186741]
56. Hughes EG, Kang SH, Fukaya M, Bergles DE. Oligodendrocyte progenitors balance growth with self-repulsion to achieve homeostasis in the adult brain. Nat Neurosci. 2013; 16:668–76. [PubMed: 23624515]
57. Kondo T, Raff M. Oligodendrocyte precursor cells reprogrammed to become multipotential CNS stem cells. Science. 2000; 289:1754–7. [PubMed: 10976069]
58. Kondo T, Raff M. Chromatin remodeling and histone modification in the conversion of oligodendrocyte precursors to neural stem cells. Genes & development. 2004; 18:2963–72. [PubMed: 15574597]
59. Noble M, Smith J, Power J, Mayer-Proschel M. Redox state as a central modulator of precursor cell function. Ann N Y Acad Sci. 2003; 991:251–71. [PubMed: 12846992]
60. Dimou L, Gallo V. NG2-glia and their functions in the central nervous system. Glia. 2015; 63:1429–51. [PubMed: 26010717]

Highlights

- Astrocyte K^+ channels are highly resistant to cerebral ischemic insults.
- Neuronal ion channels are functional in the early ischemia for spike generation.
- K^+ gradient loss is a major cause of neuronal/astrocyte depolarization in stroke.
- NG2 glia are more resilient than other CNS cells to ischemic insults.

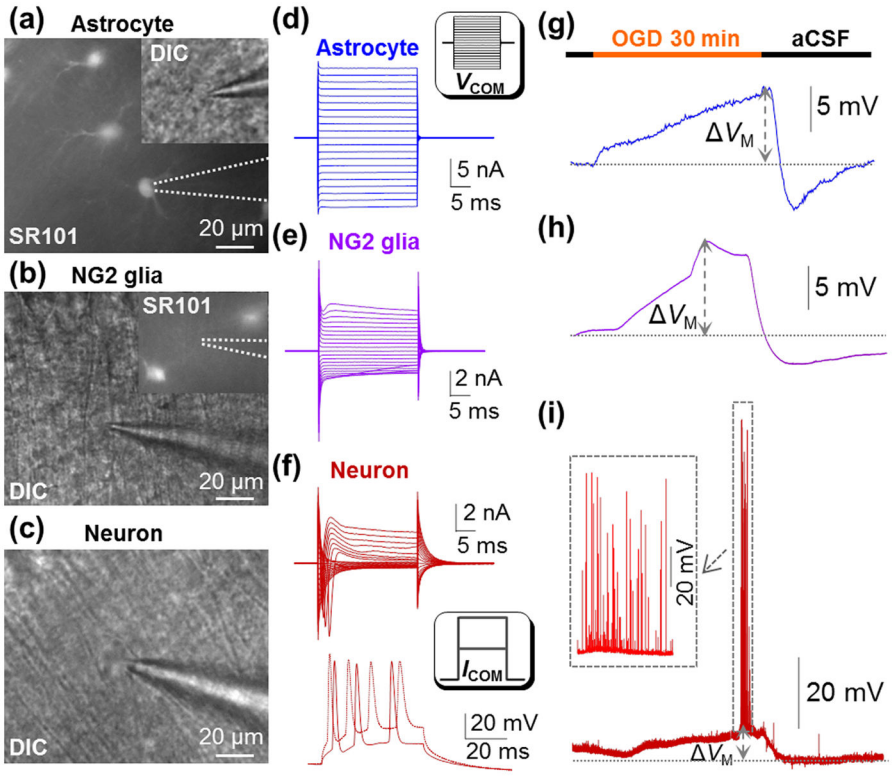

Figure 1. Electrophysiological responses of hippocampal astrocyte, NG2 glia and pyramidal neuron to OGD

(a-c) An astrocyte identified by SR101 staining, an NG2 glia devoid of SR101 staining, and a pyramidal neuron in CA1 region. (d-f) Representative whole-cell current profiles of an astrocyte, an NG2 glia, and a pyramidal neuron. Inset in (d), voltage steps (V_{COM}) were from -180 mV to +20 mV in 10 mV increments. The bottom panel in (f), action potentials induced by 100–200 pA/50 ms current pulses (I_{COM}). (g-i) A 30 min OGD-induced V_M response of three cell types. Inset in (i), the neuronal action potentials occurred and vanished during OGD-induced depolarization.

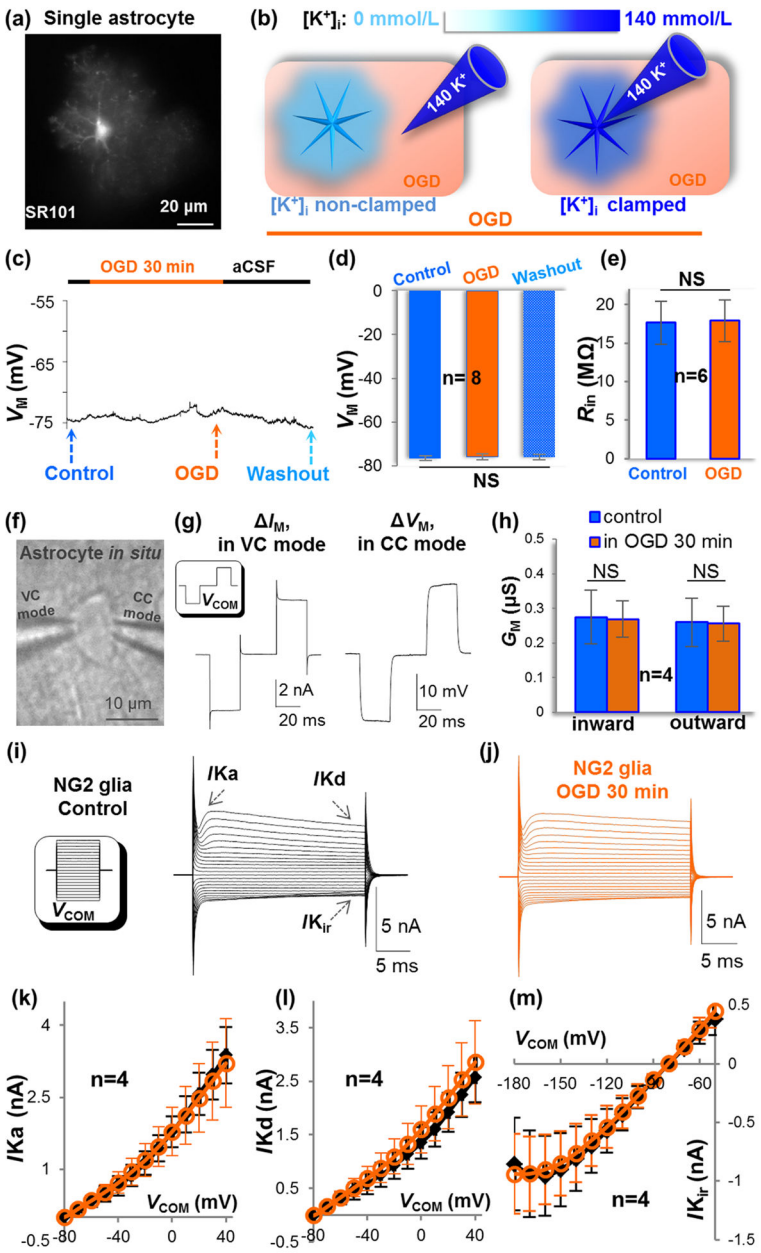

Figure 2. OGD induces no detectable damage to astrocytic and NG2 glial membrane ion channels

(a) A single freshly dissociated astrocyte stained with SR101. (b) Schematic illustration of OGD-induced K^+ gradient dissipation (left, "$[K^+]_i$ non-clamped"), and masked this $[K^+]_i$ loss due to dialysis of the cell by electrode solution (right, "$[K^+]_i$ clamped"). (c-d) Under $[K^+]_i$ clamped condition, OGD-induced depolarization was eliminated. NS: no significant difference (P>0.05, ANOVA). (e) Unchanged R_{in} in astrocyte during recording (P>0.05, paired sample t-test). (f-g) Dual patch single astrocyte recording for analysis of membrane conductance (G_M). In VC mode (left electrode), the cell was held at -80 mV. The delivered command voltages (V_{COM}) were ±50 mV/25 ms separated by 30 ms intervals. The V_{COM}-induced membrane current (ΔI_M) was recorded using the same electrode. The CC mode

(right electrode) was set in I=0 mode to record the V_{COM}-induced change in membrane voltage (ΔV_M). (g) Shows the recorded ΔV_M and ΔI_M. (h) The summary shows no OGD-induced change in astrocyte G_M (P>0.05, paired sample t-test). (i-j) Unaltered current profile of NG2 glia in control and OGD. Inset in (i), V_{COM} ranging from -180 mV to +40 mV in 10 mV increments. (k-m) The I-V plots of NG2 glial IKa, IKd, and IK$_{ir}$ before and 30 min in OGD. Current at each step was compared between control and OGD and no significant change was found in these ion channels (P>0.05, paired sample t-test).

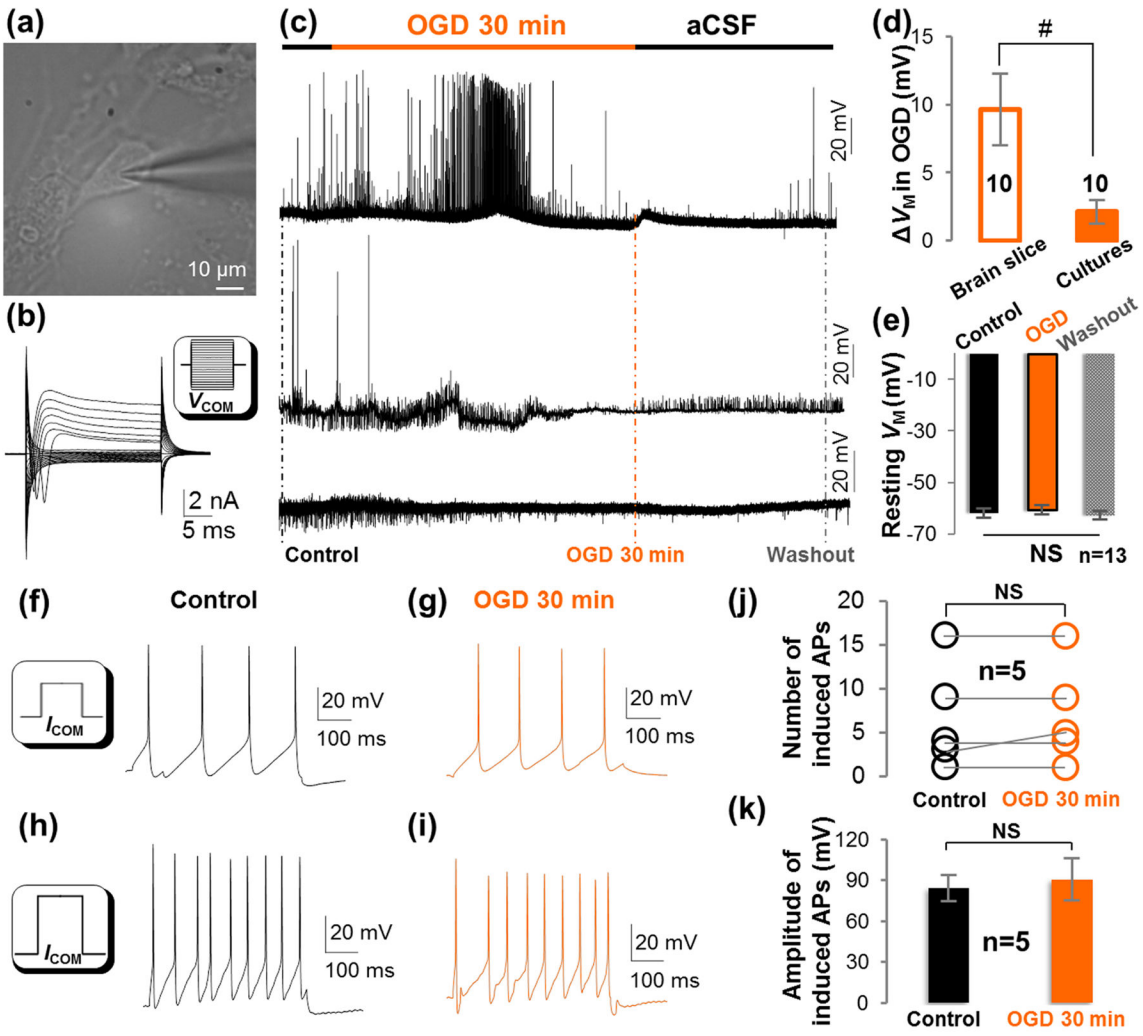

Figure 3. A short-term OGD does not alter the activity of voltage-gated ion channels or the excitability of cultured hippocampal neurons

(a-b) DIC image and a representative whole-cell current profile of a cultured hippocampal neuron. The cultured hippocampal neuron expressed voltage-gated Na^+ and K^+ current conductance as neurons in hippocampal slices. Inset in (b), V_{COM} ranging from -180 mV to +40 mV in 10 mV increments. (c) Three different patterns of neuronal spontaneous firing response to OGD. (d) In 10/23 cultured neurons, OGD induced a small depolarization compared to a large neuronal depolarization in slice (#, $P<0.01$, t-test). (e) In 13/23 cultured neurons, OGD induced no detectable depolarization (NS, $P>0.05$, ANOVA). (f-i) Representative induced action potentials in control and OGD. I_{COM} in insets: 100 pA/500 ms in (f); 200 pA/500 ms in (h). (j-k) The number and amplitude of induced action potentials were not altered after 30 min OGD ($P>0.05$, paired sample t-test).

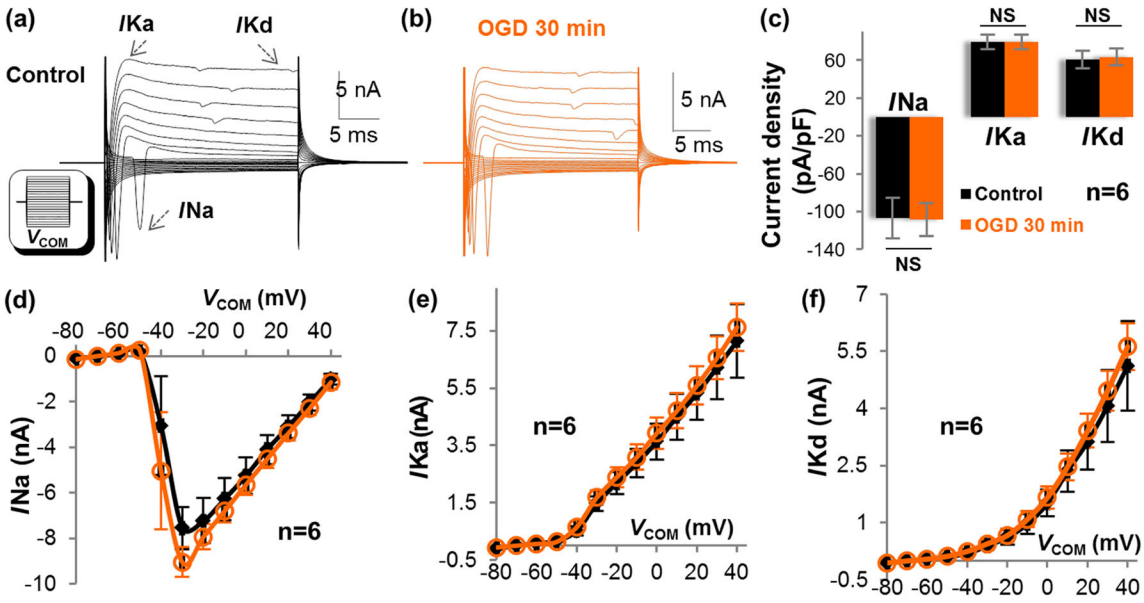

Figure 4. OGD does not alter the activity of neuronal membrane ion channels

(a-b) Representative current profiles of a cultured hippocampal neuron in control and OGD. Inset in (a), V_{COM} ranging from -180 mV to +40 mV in 10 mV increments. (c) A 30 min OGD induced no change in the current density of voltage-gated ion channels: INa at V_{COM} -30~-40 mV; IKa and IKd both at V_{COM} +40 mV (P>0.05, paired sample t-test). (d-f) The I-V plots of INa, IKa, and IKd. Current at each step was compared between control and OGD and no significant change was found in these ion channels (P>0.05, paired sample t-test).

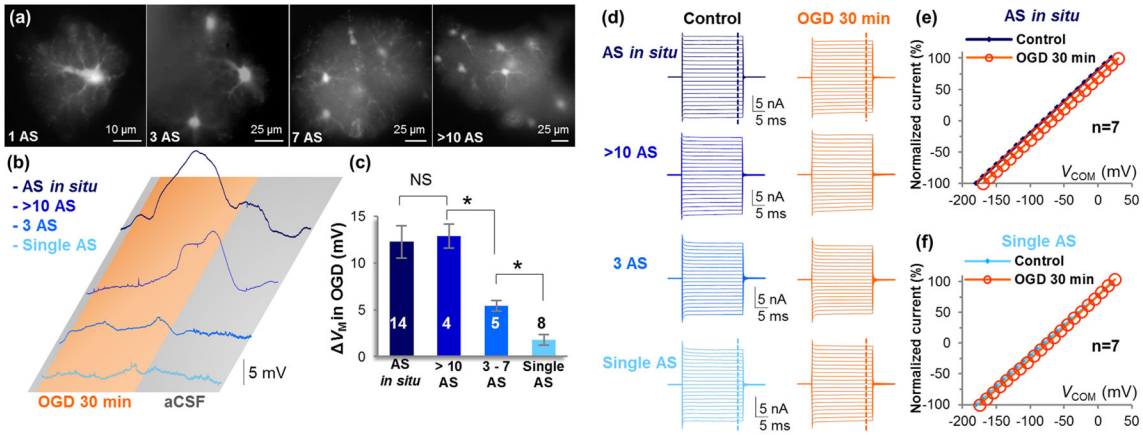

Figure 5. OGD-induced depolarization increases with more astrocytes coupling into a syncytium

(a) SR101 staining of a single freshly dissociated astrocyte, and three "miniature syncytia" with a varied number of astrocytes as indicated. AS: astrocyte. (b) OGD-induced V_M depolarization increases with the number of coupled astrocytes. (c) Quantification of OGD-induced ΔV_M in (b) (NS, $P>0.05$; *, $P<0.05$, ANOVA). (d) Representative astrocyte whole-cell currents recorded before and at the end of 30 min OGD under uncoupled and varied coupling syncytial sizes. (e) Normalized *I-V* plots show an OGD-induced positive shift in *I-V* plot (depolarization), but no suppression of passive conductance change in astrocyte *in situ*. (f) OGD induced neither a shift in *I-V* plot nor reduction in passive conductance in single astrocytes.

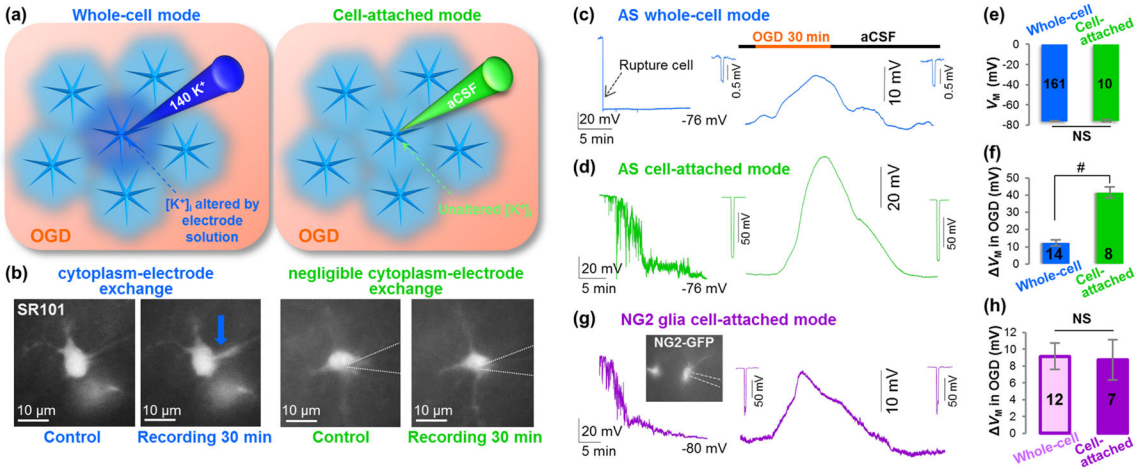

Figure 6. K^+ gradient dissipation contributes significantly to OGD-induced astrocyte depolarization

(a) Schematic diagram of conventional whole-cell mode (left), and cell-attached mode (right) for V_M recording in syncytial-coupled astrocytes. (b) SR101 fluorescence in recording electrode shows cytoplasm-electrode exchange in whole-cell mode (blue arrow), but not in cell-attached mode. (c-d) Representative V_M recording in whole-cell mode (c) and in cell-attached mode (d) of astrocytes *in situ*. Insets show unchanged R_{in}. (e) Quantification of V_M shows no significant difference of the V_M recorded in whole-cell and cell-attached modes ($P>0.05$, *t*-test). (f) The OGD-induced astrocytes ΔV_M is significantly greater in cell-attached mode than in whole-cell mode ($P<0.01$, *t*-test). (g) Representative V_M recording of NG2 glia in cell-attached mode. Insets show unchanged R_{in}. (h) The OGD-induced NG2 glia ΔV_M is comparable in cell-attached mode and in whole-cell mode ($P>0.05$, *t*-test).

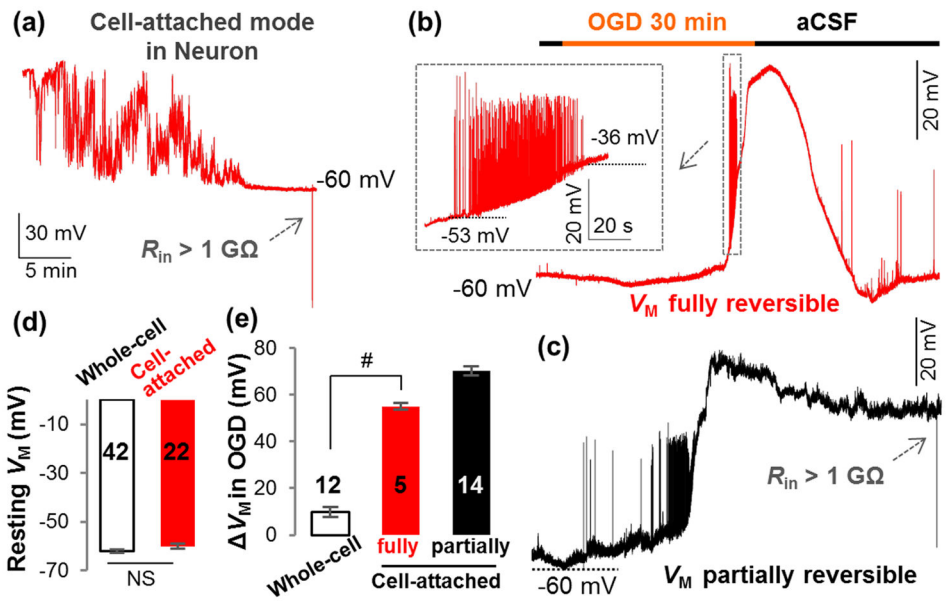

Figure 7. K^+ gradient dissipation contributes significantly to OGD-induced neuronal depolarization

(a) Cell-attached V_M recording from a hippocampal pyramidal neuron *in situ*. Two types of V_M responses to OGD are shown in (b) (fully reversible) and (c) (partially reversible). Inset in (b), the neuronal action potentials occurred and vanished during OGD-induced depolarization. (d) The resting V_M recorded in cell-attached (a) and conventional whole-cell modes are comparable in pyramidal neurons (P>0.05, t-test). (e) For the neurons with fully reversible V_M, OGD-induced depolarization (ΔV_M) was significantly greater in cell-attached mode than that of whole-cell mode (P<0.01, t-test). The OGD-induced depolarization from neurons with partially reversible V_M is shown in a separate column in (e) but was not included in the statistical comparison.